Research Report
KTC-07-08/FRT118-07-1F

KENTUCKY TRANSPORTATION CENTER

RETROFIT OF THE LOUISA-FORT GAY BRIDGE USING CFRP LAMINATES

UNIVERSITY OF KENTUCKY
College of Engineering

OUR MISSION

We provide services to the transportation community through research, technology transfer and education. We create and participate in partnerships to promote safe and effective transportation systems.

OUR VALUES

Teamwork
Listening and communicating along with courtesy and respect for others.

Honesty and Ethical Behavior
Delivering the highest quality products and services.

Continuous Improvement
In all that we do.

Research Report
KTC-07-08/FRT118-03-1F

Retrofit of the Louisa-Fort Gay Bridge using CFRP Laminates

by

Ching Chiaw Choo
Post-doctoral Research Associate, Kentucky Transportation Center
University of Kentucky

Tong Zhao
Structural Engineer
Structus, Inc., San Francisco, CA
(Formerly Visiting Professor, Kentucky Transportation Center)
and

Issam E. Harik
Professor of Civil Engineering and Program Manager, Structures and Coatings,
Kentucky Transportation Center
University of Kentucky

Kentucky Transportation Center
College of Engineering, University of Kentucky

in cooperation with

Transportation Cabinet
Commonwealth of Kentucky

and

Federal Highway Administration
U.S. Department of Transportation

The contents of this report reflect the views of the authors who are responsible for the facts and accuracy of the data presented herein. The contents do not necessarily reflect the official views or policies of the University of Kentucky, the Kentucky Transportation Cabinet, nor the Federal Highway Administration. This report does not constitute a standard, specification or regulation. Manufacturer or trade names are included for identification purposes only and are not to be considered an endorsement.

June 2007

Technical Report Documentation Page

1. Report No.	2. Government Accession No.	3. Recipient's Catalog No.
KTC-07-08/FRT118-03-1F		

4. Title and Subtitle

Retrofit of the Louisa-Fort Gay Bridge using CFRP Laminates

5. Report Date
June 2007

6. Performing Organization Code

7. Author(s): Ching Chiaw Choo, Tong Zhao, and Issam Harik

8. Performing Organization Report No.
KTC-07-08/FRT118-03-1F

9. Performing Organization Name and Address

Kentucky Transportation Center
College of Engineering
University of Kentucky
Lexington, Kentucky 40506-0281

10. Work Unit No. (TRAIS)

11. Contract or Grant No.
FRT118

12. Sponsoring Agency Name and Address

Kentucky Transportation Cabinet
State Office Building
Frankfort, Kentucky 40622

13. Type of Report and Period Covered
Final

14. Sponsoring Agency Code

15. Supplementary Notes
Prepared in cooperation with the Kentucky Transportation Cabinet and the U.S. Department of Transportation, Federal Highway Administration.

16. Abstract

This report details the processes pertaining to the repair and strengthening of the Louisa-Fort Gay Bridge, Lawrence County, KY, using advanced composite materials. Site inspections revealed flexural cracks in the reinforced concrete girders of the continuous bridge structure. To determine the cause of these cracks, an evaluation was initiated based on vehicle classification and truck weight data. The results confirmed that certain reinforced concrete girders were stressed beyond the limits allowed by the AASHTO Code. A retrofit scheme using carbon fiber reinforced polymer (CFRP) composite was devised and the amount of CFRP laminates needed for flexural strengthening was determined from moment-curvature analyses. Retrofitting work began in September of 2003, and the project was completed in October of 2003. Crack gauges were installed at the affected areas to monitor the effectiveness of the retrofit. The bridge was inspected on a number of occasions and, as of September 28 2006, no movement in the crack gauges has been observed.

17. Key Words	18. Distribution Statement
advanced composites, flexural cracks, overload, retrofitting, reinforced concrete girder, allowable stress limits	Unlimited with approval of Kentucky Transportation Cabinet

19. Security Classif. (of this report)	20. Security Classif. (of this page)	21. No. of Pages	22. Price
Unclassified	Unclassified	34	-

Form DOT 1700.7(8-72) **Reproduction of Completed Page Authorized**

TABLE OF CONTENTS

LIST OF FIGURES

EXECUTIVE SUMMARY

Routine inspection of the Louisa-Fort Gay Bridge revealed that flexural cracks have formed in the continuous reinforced concrete girders in the positive bending regions. In order to characterize the existing service load conditions of the bridge, vehicle classification and truck weight data were collected and analyzed. It was concluded that the trucks that were concurrently operating and traversing the bridge may have been carrying loads exceeding the legal weight limit. Further evaluation confirmed that most of the reinforced concrete girders were stressed beyond the allowable service limits specified by the American Association of State and Highway Transportation Official (AASHTO) Specification. In order to accommodate excessive service loads, as well as to extend the service life of the bridge, recommendations were to use carbon fiber reinforced polymer (CFRP) laminates to retrofit the reinforced concrete girders. A detailed moment-curvature analysis was carried out to establish the appropriate amount of laminates required for flexural strengthening. The retrofit was implemented in September of 2003 and the project was completed in October of 2003. Crack gauges were installed at critical crack locations to monitor the effect of the retrofit. As of September 28 2006, no crack movement has been observed.

ACKNOWLEDGMENTS

Financial support for this project was provided by the Federal Highway Adminstration and the Kentucky Transportation Cabinet under the Innovative Bridge Research and Construction Program – IBRC (Grant FRT118). The authors would like to thank Mr. David Steele with the Kentucky Transportation Cabinet for his guidance throughout this project. The authors also wish to express their gratitude to Mr. Scott Pabian and Mr. Abheetha Peiris for their contribution in completing this project.

1. INTRODUCTION

1.1 The Louisa-Fort Gay Bridge

The Louisa-Fort Gay Bridge is located in the small mining community of Lawrence County, Kentucky. The bridge was constructed in 1979. The bridge is a 12-span continuous bridge structure consists of composite concrete deck-steel girder spans and reinforced concrete middle spans that comprise an intersection for traffic coming from three different directions. A schematic plan view of the reinforced concrete spans (Spans 4-5-6-7) of the bridge is shown in Fig. 1.1.

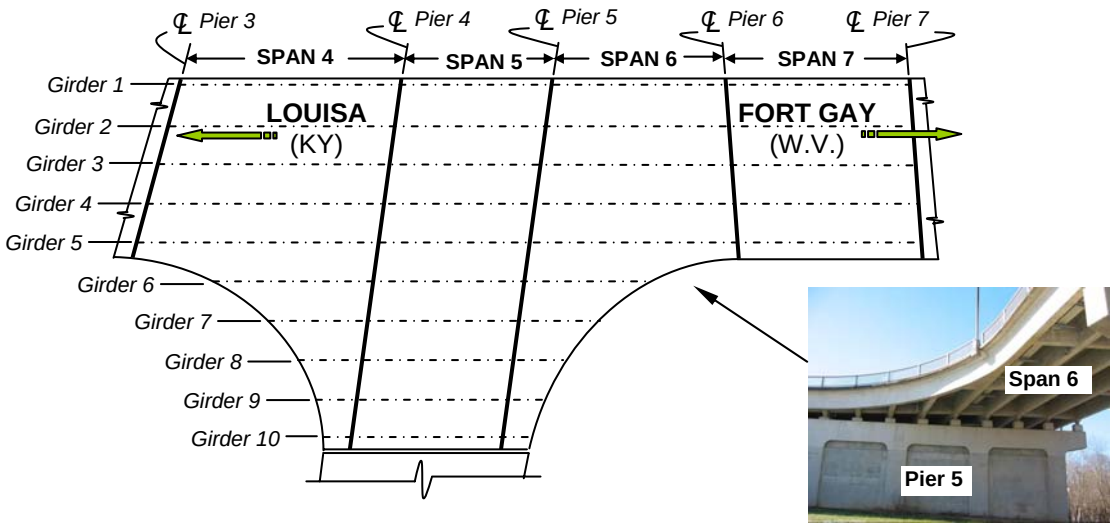

Fig. 1.1 – The continuous reinforced concrete middle spans of the Louisa-Fort Gay Bridge.

1.2 Cracks in Reinforced Concrete Girders

A routine inspection revealed cracks in the reinforced concrete girders in Spans 4, 6 and 7. These cracks were visible at ground elevation. Fig. 1.2 shows the view of the concrete spans and the estimated height of the superstructure from the ground elevation. Fig. 1.3 shows the cracks that had developed at the bottom web of a typical reinforced concrete girder of the bridge. These cracks formed primarily due to high flexural stresses that developed in the positive bending regions of the continuous structure.

(a) Spans 5, 6 and 7.

(b) Spans 4 and 5

Fig. 1.2 – The continuous reinforced concrete middle spans of the Louis-Fort Gay Bridge.

(a) Flexural crack in one of the girder

(b) Close-up of a flexural crack

Fig. 1.3 – Flexural cracks observed in Spans 4, 6 and 7 (see Fig. 1.2).

1.3 Objective

In this report, the strengthening and repair of the Louisa-Fort Gay Bridge is detailed. The objective of this project is to demonstrate that the use of high-strength carbon fiber reinforced polymer (CFRP) composite laminates can be an efficient and effective way of retrofitting the bridge elements by improving their respective strength and stiffness. It is also expected that such repair will extend the service life of the bridge.

1.4 Tasks

In order to achieve the objective of this study, the following tasks were carried out:

Task 1 Detailed Evaluation: A detailed evaluation was performed to determine a satisfactory repair using CFRP laminates. The appropriate amount of the CFRP laminates needed to strengthen the existing girders was quantified using the moment-curvature analysis. Details of the analysis are included in this report.

Task 2 Construction: The Construction phase of the project is presented herein. The repair, which involved crack repair, surface preparation, and CFRP laminate application, began in September 2003, and was completed in October 2003.

Task 3 Post-repair Monitoring: Crack gauges were installed at critical crack locations to monitor the effect of the retrofit. Inspections were scheduled on a regular basis and continued for a period of 3 years after the repair.

2. DETAILED EVALUATIONS

2.1 Truck Types

Vehicle classification and truck weight data were collected for the evaluation process. Fig. 2.1 shows the schematics of various truck types that were traversing the bridge. Fig. 2.1.c shows the legal truck weight of a typical Type 9 truck. Fig. 2.4.d shows the estimated weight that a Type 9 truck was actually carrying based on weigh-in-motion (WIM).

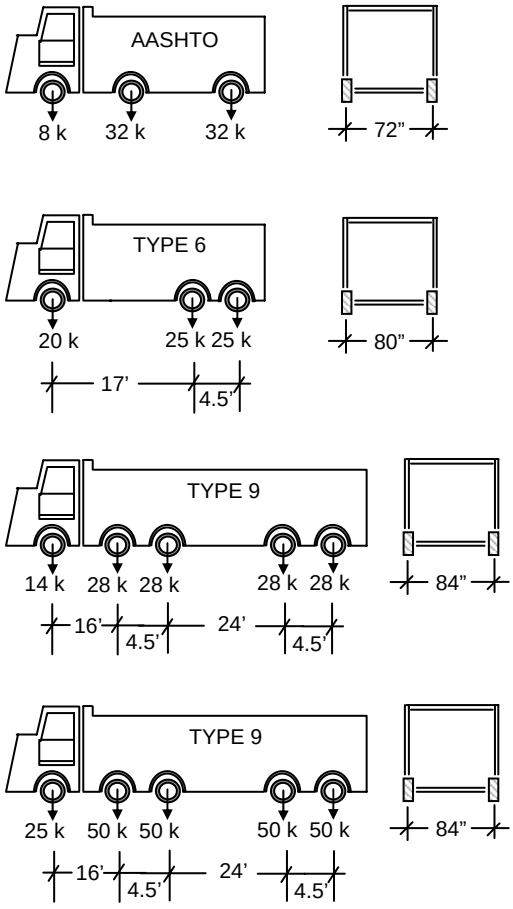

(a) AASHTO Truck HS20-44
[Total weight = 72 k]

(b) Type 6 Coal Truck
[Total weight = 70 k]

(c) Type 9 Coal Truck (Legal)
[Total weight = 126 k]

(d) Type 9 Coal Truck (WIM)
[Total weight = 225 k]

Fig. 2.1 – Truck type and loading that cross the Louisa-Fort Gay Bridge.

2.2 Finite Element Analysis

To investigate the effects of various truck types shown in previous section, analytical investigation was carried out. The process first involved the creation of a finite element model of reinforced concrete middle spans of the bridge. In this study, the reinforced concrete middle spans were constructed using SAP2000 (Wilson 2000). For live load analysis, one single truck, without any additional traffic or lane loads, was considered in the live load analysis.

The moments generated from the loading, particularly ones in the positive bending regions, were distributed to the respective girders based on the live load distribution factors computed for the parallel girders. Live load distribution factor computations are presented in Appendix A. The bending moments both at service and at ultimate conditions of respective girders were generated and tabulated in Appendix B.

2.3 Moment-Curvature Analysis

The flexural capacity of the reinforced concrete girders was determined from a moment-curvature analysis procedure. The moment-curvature (M_n-ϕ) relation captures the basic load-deformation characteristics of a given girder under bending action. Different stress or load levels (i.e. allowable service stresses as defined in AASHTO or other code provisions) were identified once the moment-curvature characteristics of the reinforced concrete members were generated.

Typically, the moment-curvature relation of a reinforced concrete girder section can be derived based on stress equilibrium, strain compatibility, and material constitutive laws. The following assumptions were used in the formulation of the moment-curvature analysis:

- Strain distribution is linear throughout the beam section;
- Perfect bond exists between the concrete and any reinforcement (steel and externally bonded CFRP laminates);
- The tensile strength of concrete is ignored;

- Failure of the beam occurs when either the compressive strain in the concrete reaches 0.003 or the strain in the outermost layer of tension steel reaches its ultimate (e.g., ε_u = 0.10, typical for mild steel). For reinforced concrete girder strengthened with CFRP laminates, there is a possibility of tensile rupture (ε_{ft} = ε_{fut} = 0.0168, refer to Fig. C.1) of the laminates prior to concrete reaching 0.003. It should be noted that since ε_{fut} is much smaller than ε_u, the rupture of the CFRP laminates would occur prior to the outermost tension steel reaching its ultimate. In this case, once the failure of the strengthened beam is initiated it would, in general, revert back to the behavior of un-strengthened beam (refer to Appendix B).

The schematic in Fig. 2.2 shows how the bending strength (M_n) and curvature (ϕ) are computed for a typical beam section using an assumed linear strain distribution:

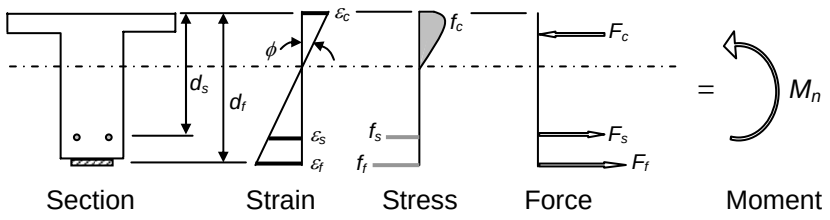

Fig. 2.2 – Moment-curvature computation of typical beam section.

Based on equilibrium conditions, strain compatibility, and material constitutive laws, the full range of moment-curvature (M_n-ϕ) responses can be generated for a beam section (either the original or the strengthened section). In general, the process can be summarized as follows:

(1) Select a small value for the concrete strain, ε_c, at the outmost concrete fiber in compression.
(2) Assume the location of the neutral axis.
(3) From linear strain distribution, determine the strains in all reinforcement (e.g. steel and FRP).

(4) Using concrete and reinforcement stress-strain relations, determine the stresses, (and consequently) the forces, of the concrete and reinforcement.

(5) Compute the resultant axial force of the section. Iterate steps 2 to 5 until the resultant axial force converges to zero (equilibrium of forces).

(6) Compute the moment or bending resistance (M_n) of the section and the corresponding curvature (ϕ).

(7) Repeat steps 1 through 6 until ε_c reaches its pre-determined ultimate strain (ε_{cu}) in compression; herein the ultimate concrete compressive strain is the ACI maximum usable strain of 0.003, or the outermost layer of tension steel reaching its ultimate ($\varepsilon_s = \varepsilon_u$).

It should be noted that for the beams in Spans 4, 5, 6 and 7, failure in the un-strengthened beam resulted from $\varepsilon_c = \varepsilon_{cu}$. For strengthened beams with CFRP laminates, the laminates reach ε_{fut} prior to ε_c reaching ε_{cu} or ε_s reaching ε_u. As previously indicated, following the rupture of CFRP laminates, the beam behaves as an un-strengthened beam and failed when ε_c reached ε_{cu}.

Unless all loads on a member, including self-weight, can be removed prior to the installation of an FRP system, the substrate to which the FRP is applied will be strained. The initial strain, ε_{fi}, which exists when all possible loads are to be considered during the FRP application process were accounted for in this project. The initial strain level, due primarily to the self-weight of the structural members, can be determined from elastic analysis of the member and can be identified on the moment-curvature curve of the original member. Let ε_f be the strain at the FRP level (Fig. 2.5) of the strengthened beam section, defined as:

$$\varepsilon_f = \varepsilon_{fi} + \varepsilon_{ff} \tag{2.1}$$

As indicated previously, there is a possibility that tensile rupture of CFRP laminates could occur prior to concrete reaching its pre-defined limiting strain of 0.003. In that case, upon tensile rupture, the load-deformation characteristics of the strengthened

member would revert back to the behavior shown for an un-strengthened beam section. However, strengthening with CFRP laminates is such that it would ensure that the beam has ample strength to resist the anticipated overload as presented in the section to follow.

2.4 Design Recommendations

Finite element and moment-curvature analyses were carried out for each girder cross-section as the beams for Spans 4, 5, 6, and 7 have different design layout due to the difference in geometry and loading in the original design. The results indicate that many of the reinforced concrete girders, except for Span 5, were stressed beyond the specified allowable permitted by AASHTO Code to varying degrees [ranging from 2% to 16% (refer to results in Appendix B)].

The amount of CFRP laminates needed to strengthen the beams was determined via moment-curvature analyses. Fig. 2.3 shows the amount of CFRP laminates, produced by Sika Corporation, required for flexural strengthening. Moment-curvature analysis was necessary in determining the appropriate amount of material required, since the ultimate strength of the retrofitted sections was dictated by FRP rupture (refer to results in Appendix B).

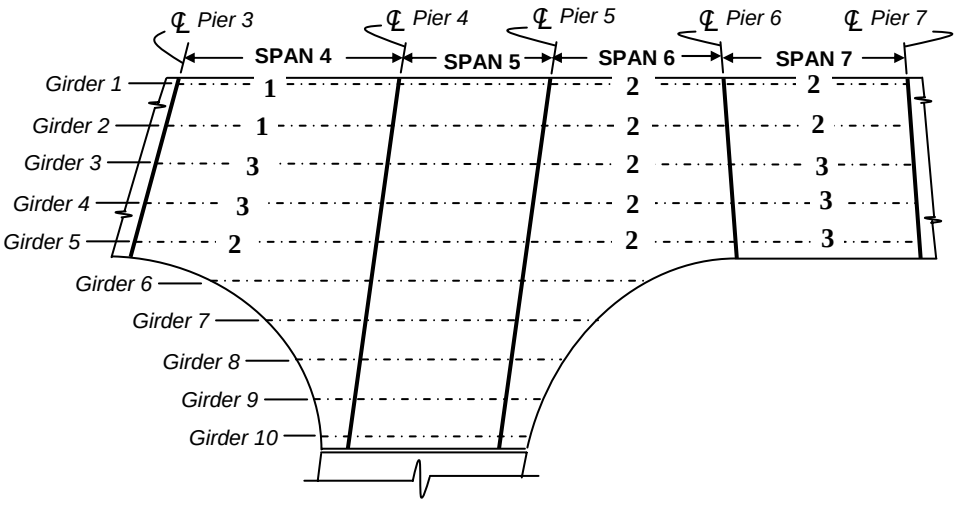

Fig. 2.3 – CFRP laminates required for beam strengthening.

(No strengthening is required for girders in Span 5)

It should be noted that all of the girders in Span 5 were excluded from this retrofit procedure because these girders were determined to possess sufficient strength as to resist actual service loads. Girders 6 to 10 of Spans 4 and 6 were also excluded from strengthening for the same reason.

3. CONSTRUCTION PHASE

3.1 Introduction

The Louisa-Fort Gay retrofitting project began in September 2003 and was completed in October 2003. The sections to follow describe the work involved in the retrofitting process: (1) surface preparation, and (2) application of the CFRP laminates.

3.2 Surface Preparation

Surface preparation ensures the cleanliness and soundness of the affected areas where bond is critical. The affected areas of selected girders were ground and cleaned to remove all loose concrete particles, debris, and other contaminants that would have affected the bond between the laminates and the concrete substrate. In addition, concrete pull-out tests (ACI 503 1992) were conducted on the concrete substrate of each girder to ensure sufficient tensile strength. In accordance with the ACI code, all affected concrete surfaces were required to possess a minimum strength of 200 psi to ensure successful bonded application of laminates. The surface grinding process is shown in Fig. 3.1. It should be noted that the surface preparation process generally involved light-weight hand-tools (i.e. surface grinder, pressure blower, etc) and only required minimal labor (Fig. 3.1).

Fig. 3.1 – Preparing concrete substrate for CFRP laminates.

3.3 Application of CFRP Laminates

The application of CFRP laminates involved the following phases: (1) applying the mixed epoxy onto the concrete with a trowel or spatula to a specified thickness, (2) applying the mixed epoxy onto the CFRP laminates; (3) placing the CFRP laminates to the affected concrete surfaces; (4) pressing the CFRP laminates using a hard-roller until adhesive is forced out on both sides; and (5) removing excess adhesive. Clamps were used in various locations along the girders to secure the CFRP laminates while allowing the adhesive to properly cure. Figure 3.2 shows the process of a CFRP laminate being attached to a reinforced concrete girder. Completed retrofitting work of Spans 4 and 6 are shown in Fig. 3.3.

Fig. 3.2 – Application of CFRP laminate to RC girder.

(a) Span 6 of the middle reinforced concrete span

(b) Span 4 of the middle reinforced concrete span

Fig. 3.3 – Reinforced concrete beams retrofitted with CFRP laminates.

4. Post-Repair Monitoring

4.1 Crack Monitoring

The Louisa-Fort Gay Bridge was monitored for a period of three years, following the completion of the retrofit in October 2003 for crack propagation and movement. Avongard crack gauges (Fig. 4.1) were installed at the affected areas of the girders. A crack gauge consists of two overlapping plexiglass/acrylic plates as shown in Fig. 4.1. One plate consists of a black millimeter grid over a white background; the other plate is transparent, with red crosshairs centered over the grid. Any movement of the crack will cause the crosshairs to shift away from the origin of the grid. Since the completion of the retrofit in October 2003, no crack movement has been observed.

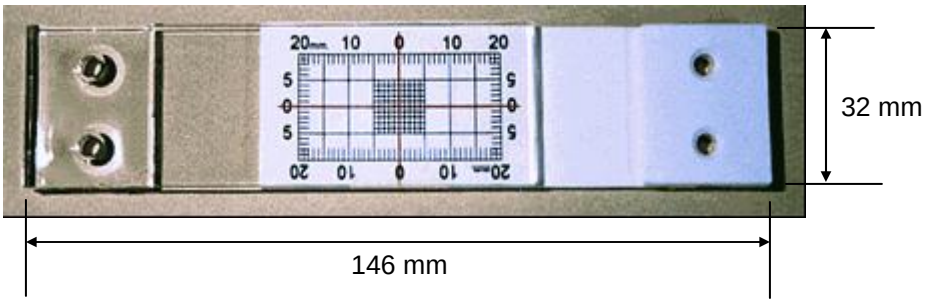

Fig. 4.1 – The Avongard crack gauge.

5. SUMMARY AND CONCLUSION

Routine inspection of the Louisa-Fort Gay Bridge revealed that flexural cracks have formed in the continuous reinforced concrete girders in the positive bending regions. In order to characterize the existing service load conditions of the bridge, vehicle classification and truck weight data were collected and analyzed. It was concluded that the trucks that were concurrently operating and traversing the bridge may have been carrying loads exceeding the legal weight limit. Further evaluation confirmed that most of the reinforced concrete girders were stressed beyond the allowable service limits specified by the American Association of State and Highway Transportation Official (AASHTO) Specification. In order to accommodate excessive service loads, as well as to extend the service life of the bridge, recommendations were to use carbon fiber reinforced polymer (CFRP) laminates to retrofit the reinforced concrete girders. A detailed moment-curvature analysis was carried out to establish the appropriate amount of laminates required for flexural strengthening. The retrofit was implemented in September of 2003 and the project was completed in October of 2003. Crack gauges were installed at critical crack locations to monitor the effect of the retrofit. As of September 28 2006, no crack movement has been observed.

References

ACI 440. 2002. Guide for the design and construction of externally bonded FRP systems for strengthening concrete structures. ACI 440.2R-02.

ACI. 1992. 503.1-92: Standard specification for bonding hardened concrete, steel, wood, brick and other materials to hardened concrete with a multi-component epoxy adhesive. American Concrete Institute.

Alagusundaramoorthy, P., Harik, I.E. and Choo, C.C., "Flexural Behavior of R/C Beams Strengthened with CFRP Sheets or Fabric", Journal of Composites for Construction, American Society of Civil Engineers. November 2003.

Arduini, M., Nanni, A., and Romagnolo, M., 2004, "Performance of One-Way Reinforced Concrete Slabs with Externally Bonded Fiber-Reinforced Polymer Strengthening," ACI Structural Journal, Vol. 101, No. 2, Mar.-Apr., pp. 193-201.

Chaallal, O., Shahawy, M., and Hassan, M., 2002, "Performance of Reinforced Concrete T-Girders Strengthened in Shear with Carbon fiber-Reinforced Polymer Fabrics," ACI Structural Journal, Vol. 99, No. 3, May-Jun., pp. 335-343.

Deniaud, C. and Cheng, J.J.R., 2003, "Reinforced Concrete T-Beams Strengthened in Shear with Fiber Reinforced Polymer Sheets," Journal of Composites in Construction, ASCE, Vol. 7, No. 4, pp. 302-310.

Grace, N., Ragheb, W.F., and Abdel-Sayed, G., 2004, "Strengthening of Cantilevel and Continuous Beams Using New Triaxially Braided Ductile Fabric," ACI Structural Journal, Vol. 101, No. 2, Mar.-Apr., pp. 237-244.

Mertz, D.R., Chajes, M.J., Gillespie, J.W., Kukich, D.S., Sabol, S.A., Hawkins, N.M., Aquino, W., and Deen, T.B., 2003, "NCHRP Report 503 – Application of Fiber Reinforced Polymer Composites to the Highway Infrastructures," TRB National Cooperative Highway Research Program, Washington, D.C.

Tavakkolizadeh, M. and Saadatmanesh, H., 2003, “Repair of Damaged Steel-Concrete Composite Girders Using Carbon Fiber-Reinforced Polymer Sheets,” Journal of Composites in Construction, ASCE, Vol. 7, No. 4, pp. 311-322.

Teng. J.G., Cao, S.Y., and Lam, L., 2001, “Behavior of GFRP Strengthened RC Cantilever Slabs,” Construction & Building Materials, Vol. 15, No. 7, Oct., pp. 339-349.

APPENDIX A

Live Load Analysis

This section contains information related to the determination of live load distribution factors for parallel girders of the Louisa-Fort Gay Bridge.

Interior Girders:

Concrete T-beam

Average girder spacing S = 9.5 ft (If S exceeds 10 ft, use footnote f.)

The distribution factor (*DF*) is:

DF = S / 6 (Bridge designed for two or more traffic lanes)

= 1.583

The impact factors (*I*) for different spans are:

$I = 50 / (L + 125)$

Where *L* is length, in feet, of the portion of the span that is loaded to produce the maximum stress in the member.

Then the live-load bending moment for the interior **T-girders 2 and 3** would be:

M_{L+I} = (live-load moment due to one truck) × 0.5 × (DF) × (1+ *I*)

Exterior Girders:

The distribution factors are determined by the lever rule. The ***lever rule*** is a method of static analysis. It involves a distribution of load based on the assumption that each deck panel is simply supported over the girder, except at the exterior girder, which is continuous with the cantilever. Because the load distribution to any girder other than one directly next to the point of load application is neglected, the lever rule is a conservative method of analysis.

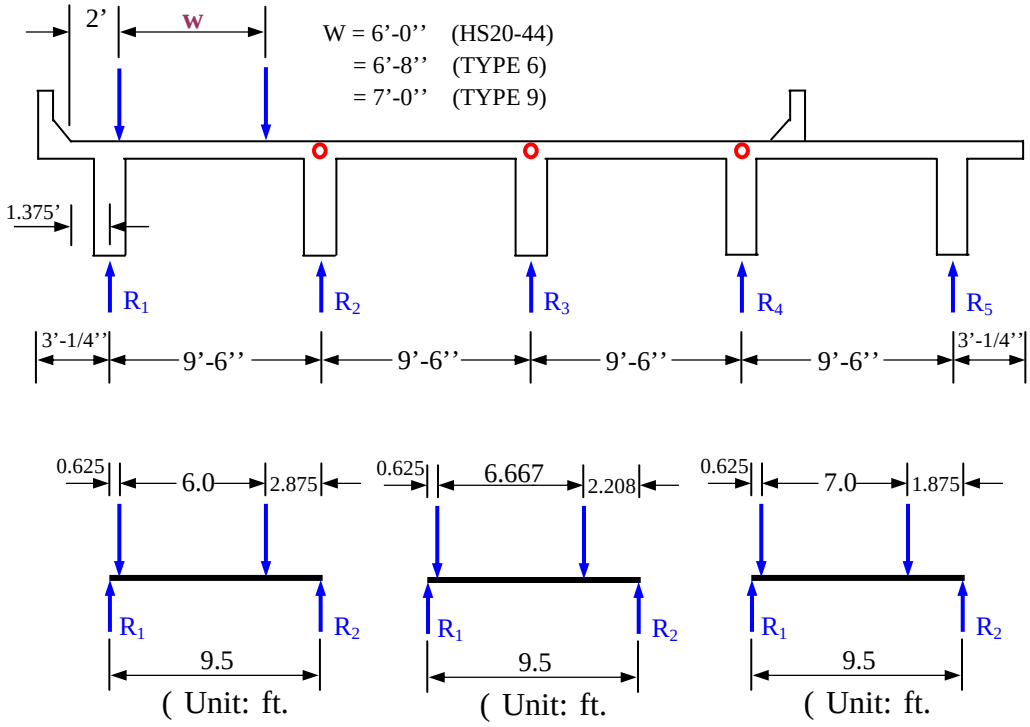

HS20-44 **TYPE 6** **TYPE 9**

$DF = R_1 = [(9.5 – 0.625) + 2.875]/9.5 = 1.237$ (HS20-44)

$= [(9.5 – 0.625) + 2.208]/9.5 = 1.167$ (TYPE 6)

$= [(9.5 – 0.625) + 1.875]/9.5 = 1.132$ (TYPE 9)

The live-load bending moment for the exterior **girder 1** and interior **girder 4** would be:

M_{L+I} = (live-load moment due to one truck) × 0.5 × (DF) × (1+*I*)

APPENDIX B

Moment-Curvature Analysis

This section contains the results of the moment-curvature analyses of the RC girders in Spans 4, 6, and 7.

Table B-1. Service loads and design loads of Section 11-11 for Girder 2 in Span 4.

Load levels	Service moments (lb-in)[1]	Design moments (lb-in)[2,3]
A. M_{DL}	14.7×10^6	19.1×10^6
B. M_{DL} & M_{LL} (AASHTO)	24.1×10^6	39.5×10^6
C. M_{DL} & M_{LL} (Type 6 – WIM)	24.3×10^6	40.0×10^6
D. M_{DL} & M_{LL} (Type 9 – LEGAL)	27.0×10^6	45.7×10^6
E. M_{DL} & M_{LL} (Type 9 – WIM)	36.6×10^6	**66.6×10^6**

[1] Refer to **Fig B.1.a** [2] Refer to **Fig B.1.b** [3] bold numbers indicate that the factored applied loads exceed the capacity of the original section

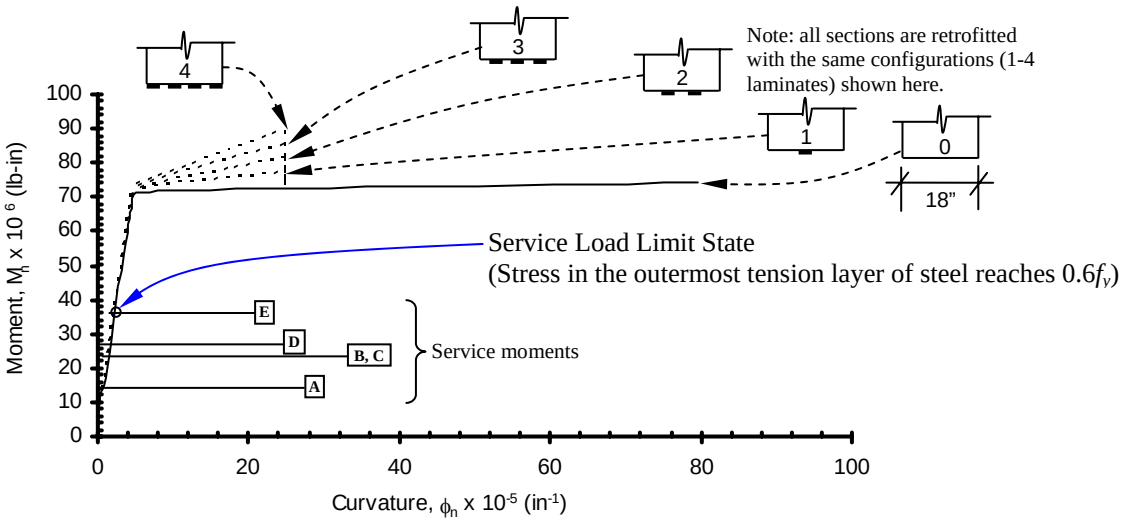

Fig. B.1.a – Comparison of service moments with M_n-ϕ_n.

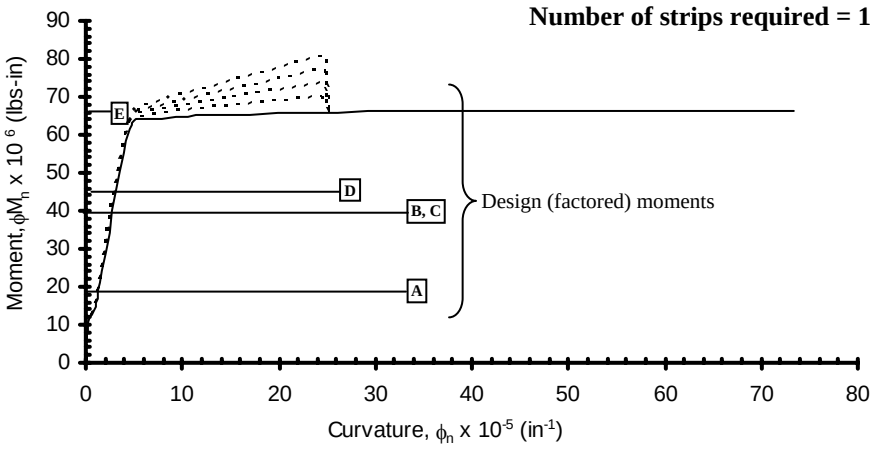

Fig. B.1.b – Comparison of design moments with ϕM_n-ϕ_n.

Table B-2. Service loads and design loads of Section 15-15 for Girder 3 in Span 6.

Load levels	Service moments (lb-in)[1]	Design moments (lb-in)[2, 3]
A. M_{DL}	6.4×10^6	8.3×10^6
B. M_{DL} & M_{LL} (AASHTO)	12.5×10^6	21.6×10^6
C. M_{DL} & M_{LL} (Type 6 – WIM)	12.8×10^6	22.3×10^6
D. M_{DL} & M_{LL} (Type 9 – LEGAL)	13.8×10^6	24.3×10^6
E. M_{DL} & M_{LL} (Type 9 – WIM)	19.6×10^6	**36.9×10^6**

[1] Refer to **Fig. B.2.a** [2] Refer to **Fig. B.2.b** [3] bold numbers indicate that the factored applied loads exceed the capacity of the original section

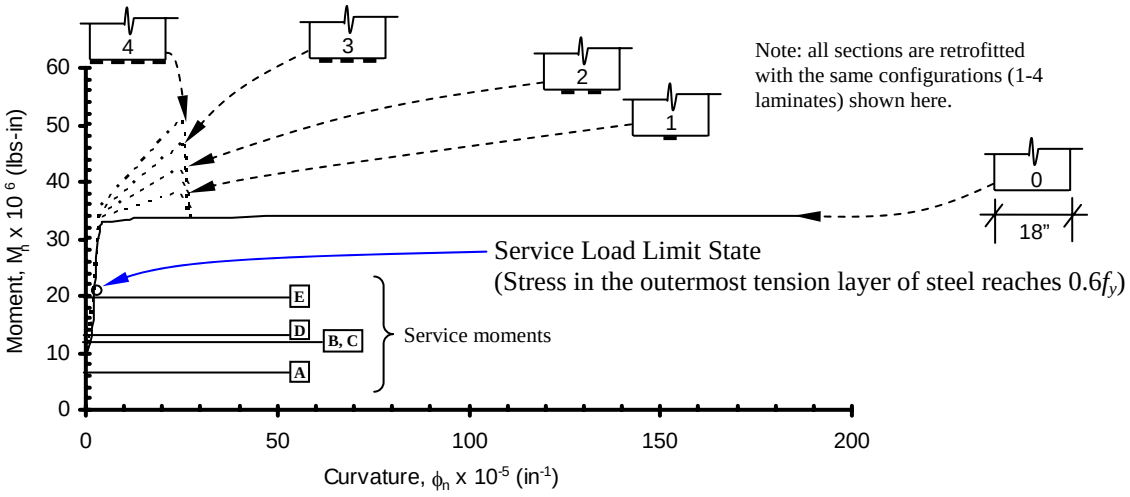

Fig. B.2.a – Comparison of service moments with M_n-ϕ_n.

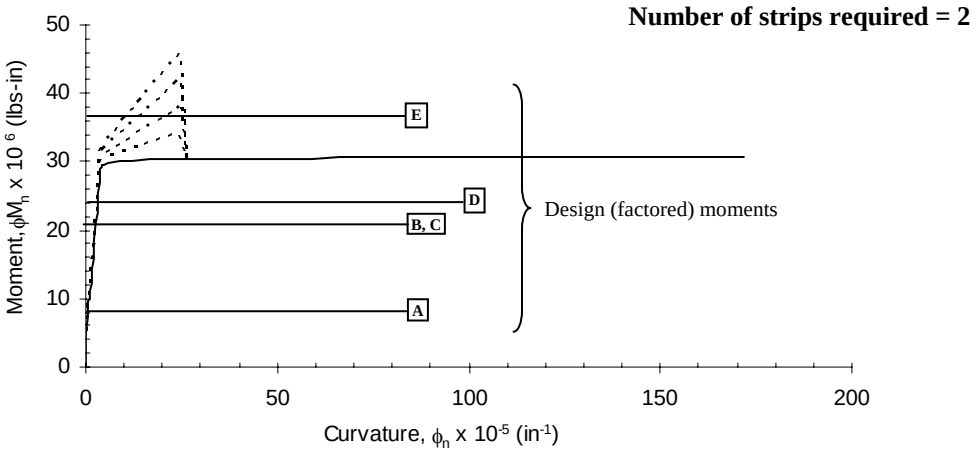

Fig. 6.b – Comparison of design moments with ϕM_n-ϕ_n.

Table B-3. Service loads and design loads of Section 17-17 for Girder 2 in Span 7.

Load levels	Service moments (lb-in)[1]	Design moments (lb-in)[2, 3]
A. M_{DL}	8.3×10^6	10.8×10^6
B. M_{DL} & M_{LL} (AASHTO)	15.7×10^6	26.8×10^6
C. M_{DL} & M_{LL} (Type 6 – WIM)	15.9×10^6	27.4×10^6
D. M_{DL} & M_{LL} (Type 9 – LEGAL)	17.1×10^6	30.0×10^6
E. M_{DL} & M_{LL} (Type 9 – WIM)	24.1×10^6	**45.0×10^6**

[1] Refer to **Fig. B.3.a** [2] Refer to **Fig. B.3.b** [3] bold numbers indicate that the factored applied loads exceed the capacity of the original section

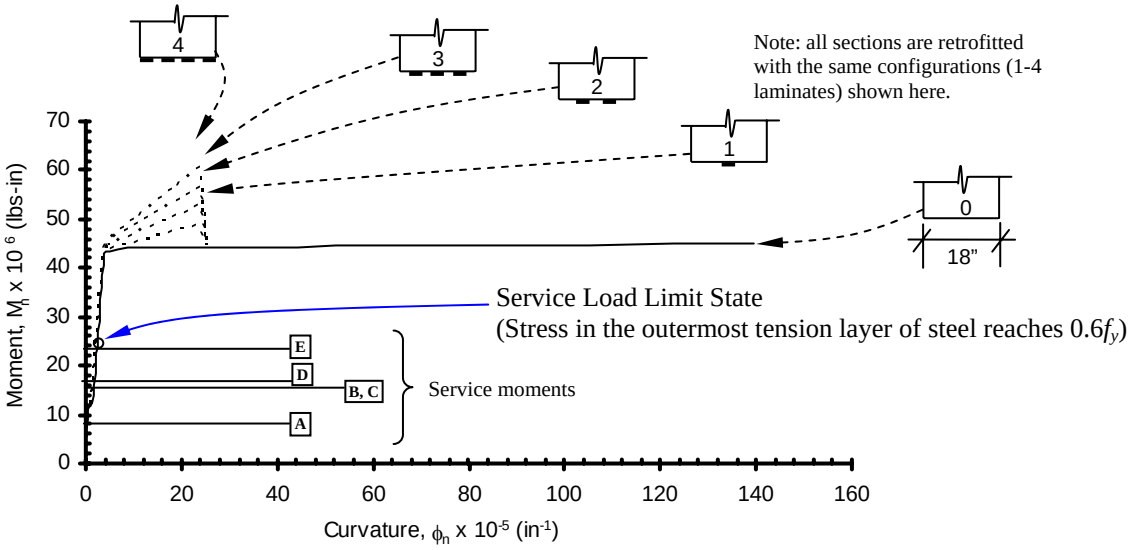

Fig. B.3.a – Comparison of service moments with M_n-ϕ_n.

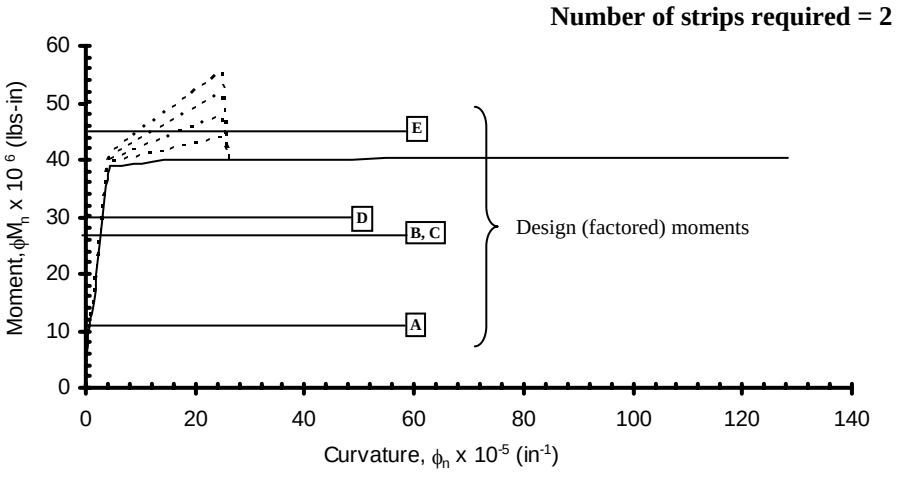

Fig. B.3.b – Comparison of design moments with ϕM_n-ϕ_n.

Table B-4. Service loads and design loads of Section 18-18 for Girder 3 in Span 4.

Load levels	Service moments (lb-in)[1]	Design moments (lb-in)[2, 3]
A. M_{DL}	15.6×10^6	20.3×10^6
B. M_{DL} & M_{LL} (AASHTO)	24.9×10^6	40.6×10^6
C. M_{DL} & M_{LL} (Type 6 – WIM)	25.2×10^6	41.1×10^6
D. M_{DL} & M_{LL} (Type 9 – LEGAL)	25.6×10^6	46.8×10^6
E. M_{DL} & M_{LL} (Type 9 – WIM)	**37.4×10^6**	**67.7×10^6**

[1] Refer to **Fig. B.4.a** [2] Refer to **Fig. B.4.b** [3] bold numbers indicate that the factored applied loads exceed the capacity of the original section

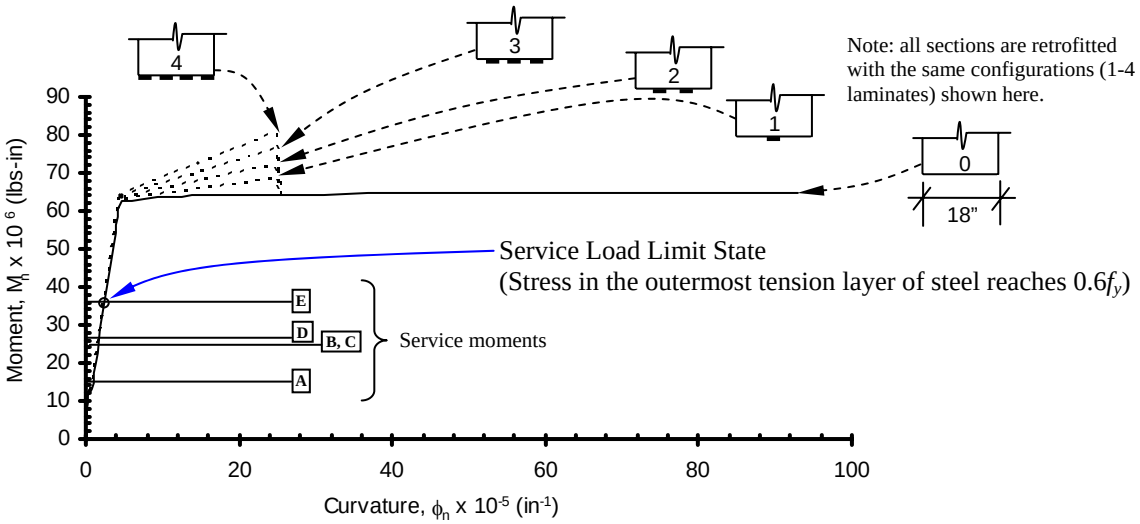

Fig. B.4.a – Comparison of service moments with M_n-ϕ_n.

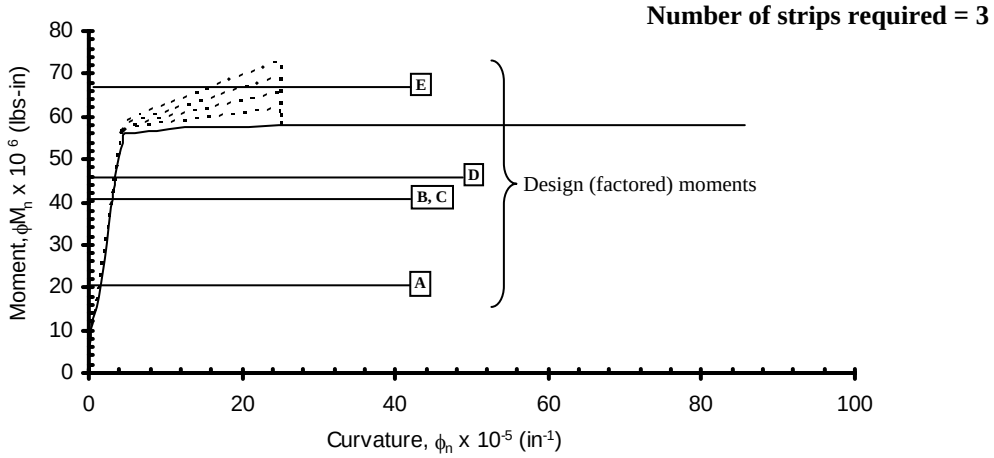

Fig. B.4.b – Comparison of design moments with ϕM_n-ϕ_n.

Table B-5. Service loads and design loads of Section 19-19 for Girder 4 in Span 7.

Load levels	Service moments (lb-in)[1]	Design moments (lb-in)[2, 3]
A. M_{DL}	9.8×10^6	12.7×10^6
B. M_{DL} & M_{LL} (AASHTO)	15.9×10^6	27.1×10^6
C. M_{DL} & M_{LL} (Type 6 – WIM)	16.2×10^6	27.7×10^6
D. M_{DL} & M_{LL} (Type 9 – LEGAL)	17.3×10^6	30.3×10^6
E. M_{DL} & M_{LL} (Type 9 – WIM)	**24.3×10^6**	**45.3×10^6**

[1] Refer to **Fig. B.5.a** [2] Refer to **Fig. B.5.b** [3] bold numbers indicate that the factored applied loads exceed the capacity of the original section

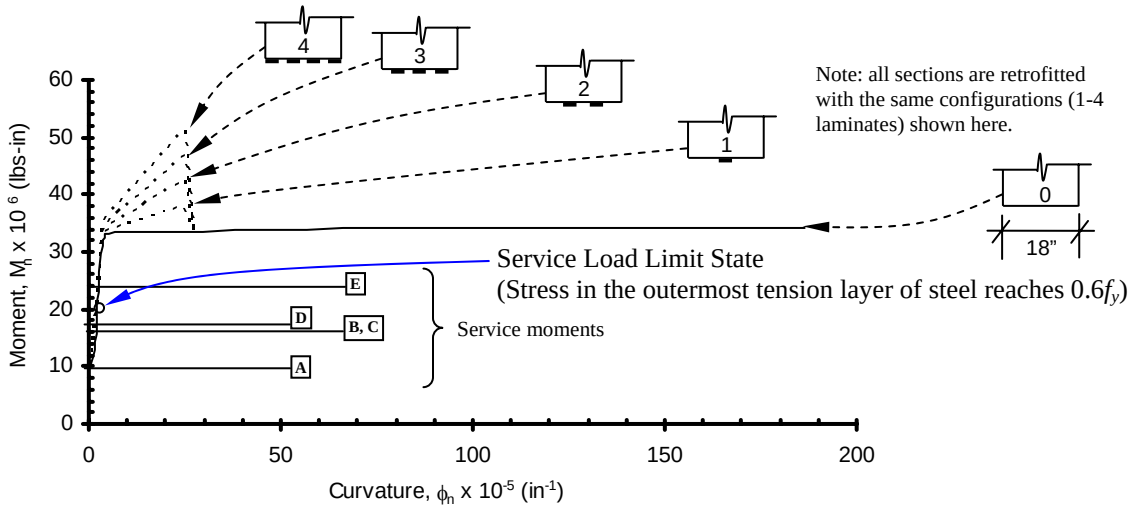

Fig. B.5.a – Comparison of service moments with M_n-ϕ_n.

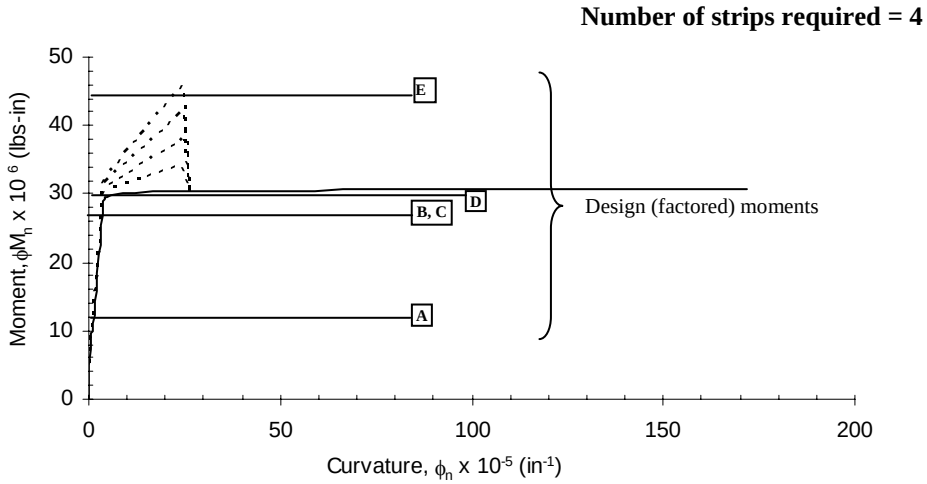

Fig. B.5.b – Comparison of design moments with ϕM_n-ϕ_n.

Table B-6. Service loads and design loads of Section 20-20 for Girder 4 in Span 4.

Load levels	Service moments (lb-in)[1]	Design moments (lb-in)[2, 3]
A. M_{DL}	16.9×10^6	22.0×10^6
B. M_{DL} & M_{LL} (AASHTO)	24.2×10^6	37.8×10^6
C. M_{DL} & M_{LL} (Type 6 – WIM)	23.9×10^6	37.3×10^6
D. M_{DL} & M_{LL} (Type 9 – LEGAL)	25.6×10^6	40.9×10^6
E. M_{DL} & M_{LL} (Type 9 – WIM)	**32.5×10^6**	**55.9×10^6**

[1] Refer to **Fig. B.6.a** [2] Refer to **Fig. B.6.b** [3] bold numbers indicate that the factored applied loads exceed the capacity of the original section

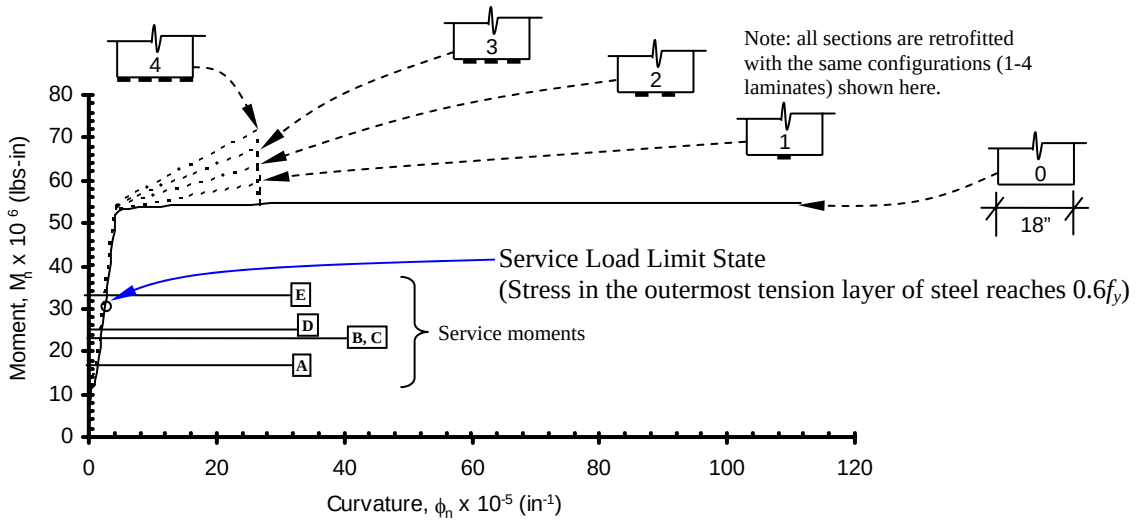

Fig. B.6.a – Comparison of service moments with M_n-ϕ_n.

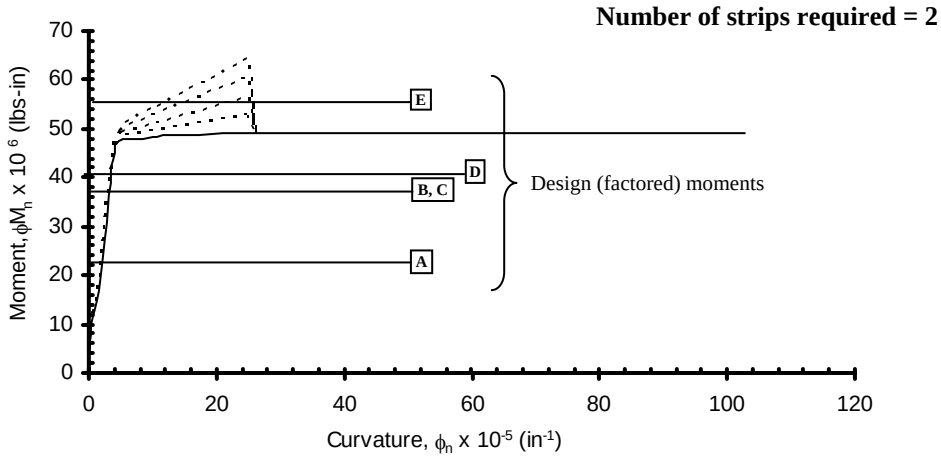

Fig. B.6.b – Comparison of design moments with ϕM_n-ϕ_n.

APPENDIX C

Carbon Fiber Reinforced Polymer (CFRP) Laminate

This section contains information related to CFRP laminates used in the strengthening process.

CFRP laminates produced by Sika were used in the project. The following are the properties of Sika CarboDur® laminate, used for flexural strengthening:

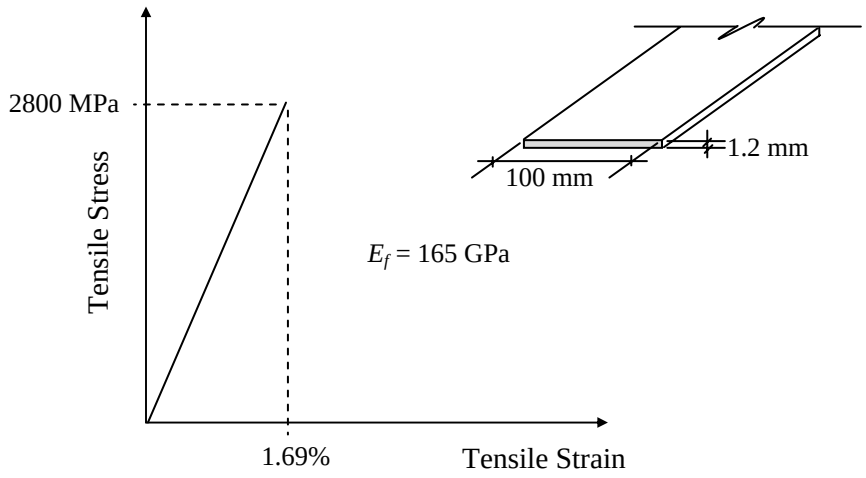

Fig. C.1: Physical and mechanical properties of CFRP laminate used for flexural strengthening.

For more information or a complete publication list, contact us at:

KENTUCKY TRANSPORTATION CENTER

176 Raymond Building
University of Kentucky
Lexington, Kentucky 40506-0281

(859) 257-4513
(859) 257-1815 (FAX)
1-800-432-0719
www.ktc.uky.edu
ktc@engr.uky.edu

The University of Kentucky is an Equal Opportunity Organization